Article

pubs.acs.org/Biomac

Rational Design of MMP Degradable Peptide-Based Supramolecular Filaments

Yi-An Lin,[†,‡] Yu-Chuan Ou,[†] Andrew G. Cheetham,[†,‡] and Honggang Cui*[,†,‡]

[†]Department of Chemical and Biomolecular Engineering and [‡]Institute for NanoBiotechnology, The Johns Hopkins University 3400 North Charles Street, Baltimore, Maryland 21218, United States

Supporting Information

ABSTRACT: One-dimensional nanostructures formed by self-assembly of small molecule peptides have been extensively explored for use as biomaterials in various biomedical contexts. However, unlike individual peptides that can be designed to be specifically degradable by enzymes/proteases of interest, their self-assembled nanostructures, particularly those rich in β-sheets, are generally resistant to enzymatic degradation because the specific cleavage sites are often embedded inside the nanostructures. We report here on the rational design of β-sheet rich supramolecular filaments that can specifically dissociate into less stable micellar assemblies and monomers upon treatment with matrix metalloproteases-2 (MMP-2). Through linkage of an oligoproline segment to an amyloid-derived peptide sequence, we first synthesized an amphiphilic peptide that can undergo a rapid morphological transition in response to pH variations. We then used MMP-2 specific peptide substrates as multivalent cross-linkers to covalently fix the amyloid-like filaments in the self-assembled state at pH 4.5. Our results show that the cross-linked filaments are stable at pH 7.5 but gradually break down into much shorter filaments upon cleavage of the peptidic cross-linkers by MMP-2. We believe that the reported work presents a new design platform for the creation of amyloid-like supramolecular filaments responsive to enzymatic degradation.

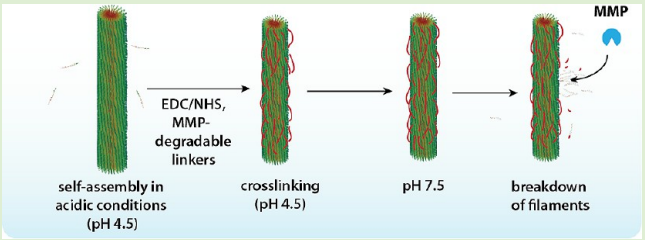

INTRODUCTION

Peptides with β-sheet forming sequences derived from, or inspired by, amyloid proteins, have been extensively incorporated into various molecular building units to construct self-assembling one-dimensional (1D) nanostructures.[1−10] These 1D amyloid-like assemblies can either serve as individual drug carriers,[7,8,11] or further entangle into a 3D network for use as hydrogels in various biomedical contexts such as protein, or cell delivery,[12,13] regenerative medicine,[14,15] tissue engineering,[3,16] cancer therapeutics,[17−19] and immune therapies.[20,21] In all cases, one challenging yet important design consideration is the selective degradation of the resulting materials by enzymes/proteases of interest. This is because chemical breakdown presents the first step toward ultimate clearance of these synthetic macromolecular/supramolecular materials once their duties are finished, and also because controlled degradation by relevant enzymes could play a critical role in regulating the release rate of the delivered cargo or in the control of cell fates such as differentiation and migration when used as extracellular matrix mimics.[22]

One current strategy is to incorporate into the molecular design a particular functional group or peptide sequence that is specific to the targeted enzymes or proteases. Although this strategy works fairly well in the design of enzyme-triggered molecular assembly into well-defined nanostructures (catalytic reactions occurring on the unassembled molecules),[23−26] only limited successes have been reported on the enzyme-induced morphological transitions[27,28] and the specific degradation of self-assembled supramolecular filaments (catalytic reactions affecting the assembled nanostructures).[29−34] In the latter cases, it is not clear whether changes in the assembled structures (both morphological transition and nanostructure degradation) stems from the cleavage reactions occurring on the nanostructures, or on the individual, unassembled molecules that leads to dissociation of the assembled structures into cleavable monomers. Specific cleavage of assembled nanostructures often proves to be challenging, mainly because enzymatic reactions in biological systems often proceed with high precision, involving specific interactions of the enzyme with its substrate in the monomeric form. These specific interactions, however, can be greatly hindered, or even prohibited once the substrates assemble into supramolecular nanostructures. Inspired by the work of Wooley and co-workers on shell-cross-linked polymeric micelles[35,36] and also the work by Xu, Epstein, and co-workers on postassembly cross-linking of peptide nanofibers,[37,38] we report herein a cross-linking strategy to construct supramolecular filaments that can specifically break down in the presence of matrix metalloprotease-2 (MMP-2). Notably, we show that the cleavage reaction actually takes place more efficiently on the degradable

Received: January 6, 2014
Revised: March 8, 2014
Published: March 10, 2014

dx.doi.org/10.1021/bm500020j | Biomacromolecules 2014, 15, 1419−1427

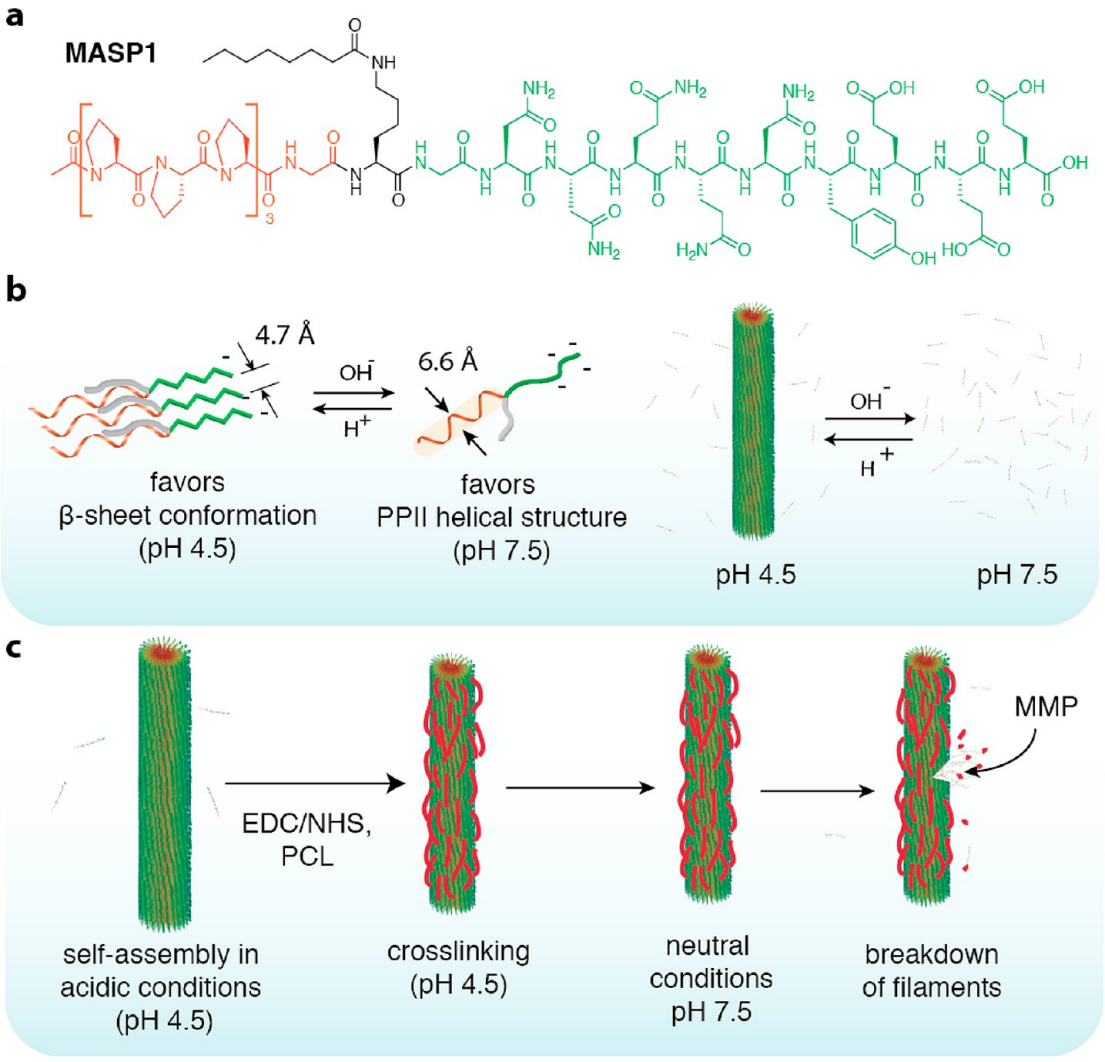

Figure 1. (a) Chemical structure of the studied molecule and (b) the key design feature of the molecular assembly principle: the reversible nature of dissociating the self-assembled 1D filaments in response to pH variation. (c) Illustration of the cross-linking strategy and the expected degradation pathway by targeted MMP. PCL represents peptide cross-linkers (PCL) containing MMP specific substrates. The designed amphiphilic peptide is expected to self-assemble into stable 1D nanostructures at a lower pH value, followed by a postcross-linking process that employs EDC/NHS chemistry and utilizes PCLs as linkers. Chemical structures of the PCL linkers are presented in Scheme 1.

linkers that stablize the assembled nanostructures, leading to the breakdown of cross-linked filaments.

MMPs are extracellular proteases that regulate a variety of physiological processes and represent key players in facilitating molecular communication between cells and their surroundings.[39] Recently, there has been a rapidly growing interest in the development of peptide-based supramolecular filaments responsive to specific MMPs due to their important biomedical applications.[27,29,30,33] Examples include the RADA peptides containing MMP-2 specific substrates by Chau et al.,[33] the self-assembling multidomain peptides developed by the Hartgerink lab (responsive to MMP-2),[30] and the self-assembling β-hairpin degrading peptides developed by Schneider, Pochan and Giano (responsive to MMP-13).[29] These researchers have shown compelling evidence that the resultant supramolecular hydrogels can break down in response to the cleavage reactions of their respective, targeted MMPs. However, since in these examples the MMP-specific sequences were incorporated into the molecular building units, their contributions to the self-assembly process may lead to difficulties in predicting the assembled morphologies as well as the mechanical properties of the resulting hydrogels. Using these systems for a different type of MMPs would require a complete redesign and characterization of the assembly system. Moreover, the formation of enzyme−substrate complexes, a critical intermediate step to facilitate the enzymatic reaction, would be affected or even suppressed if the peptide substrate is deeply embedded inside the assembled nanostructures and inaccessible to its targeted MMPs. As a result, assembly into supramolecular nanostructures would complicate the specificity of the incorporated sequence to the targeted MMPs, most likely reducing the degradation rate. Therefore, it would be advantageous to design a peptide assembly platform that could separate the assembly process (structural and morphological control) from the incorporation of MMP degradation features into supramolecular filaments (MMP responsiveness).

EXPERIMENTAL SECTION

Peptide Synthesis. All peptides used in this work were synthesized utilizing standard Fmoc solid-phase peptide chemistry on an AAPPTec Focus peptide synthesizer. In brief, for each amino acid coupling cycle, the resin first underwent Fmoc-deprotection

dx.doi.org/10.1021/bm500020j | *Biomacromolecules* 2014, 15, 1419−1427

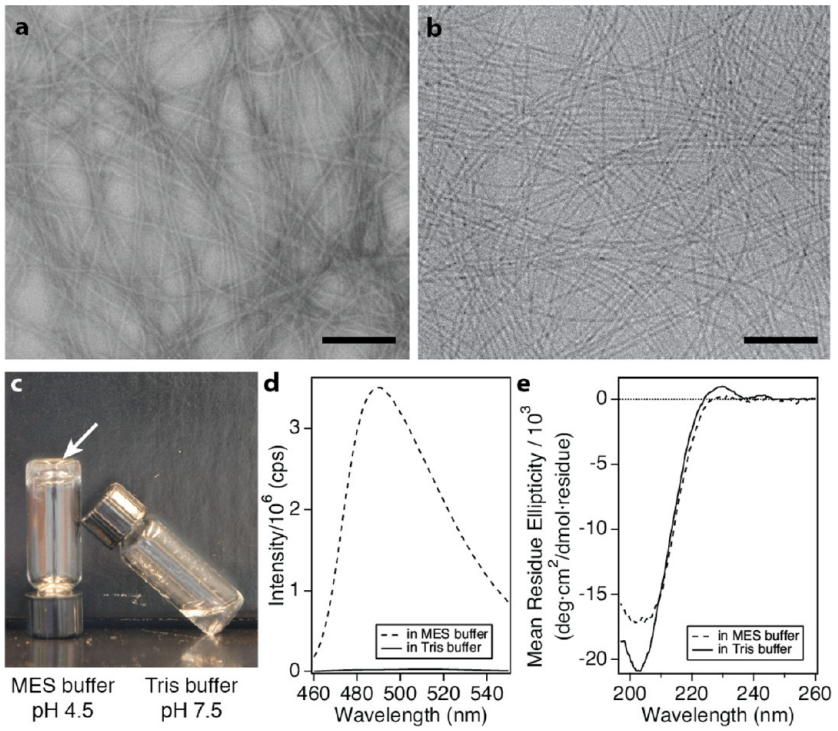

Figure 2. Molecular assembly and characterization of the design peptide. TEM (a) and cryo-TEM (b) micrographs of supramolecular filaments formed by MASP1 in MES buffer at 2.1 mM. Both bars = 200 nm. (c) Photograph of 2.1 mM MASP1 in MES buffer (pH 4.5; a self-supporting gel marked with a white arrow) and in Tris buffer (pH 7.5; a fluidic liquid). (d) Fluorescence spectra of Thioflavin T when incubated with 500 μM MASP1 in MES and Tris buffer. Concentration of Thioflavin T = 100 μM; excitation: 442 nm. (e) CD spectra of 400 μM MASP1 in MES and Tris buffer, showing strong characteristics of PPII helical secondary structure of the oligoproline.

through treatment with 20% 4-methylpiperidine in dimethylformamide (DMF), followed by reaction with a mixture of Fmoc-amino acid, *O*-benzotriazole-*N*,*N*,*N*′,*N*′-tetramethyl-uronium-hexafluorophosphate(HBTU), and diisopropylethylamine (DIEA; 4:4:6 mol equiv relative to resin) in DMF. Side chain modification of the branching lysine was performed by use of an orthogonal protecting group strategy: the ε-amine group on the branching lysine was initially protected by 4-methyltrityl (Mtt) group that can be deprotected by 3% trifluoroacetic acid (TFA), 5% triisopropylsilane (TIS) in dichloromethane (DCM), and then reacted with a mixture of acid/HBTU/DIEA (4:4:6) in DMF. The *N*-termini for all designed peptides were acetylated using 20% acetic anhydride in DMF. The cleavage of the peptides from the resin was accomplished by treating the resin with 95% TFA, 2.5% TIS, and 2.5% H_2O for 3 h. Cleaved peptides were isolated by removal of the solvents and precipitation with cold diethyl ether. Purification of the peptides was performed on a preparative HPLC column using a gradient of water and acetonitrile both containing 0.1% TFA or ammonium hydroxide. Fractions were collected and analyzed by matrix assisted laser desorption-ionization (MALDI-ToF) mass spectrometry. Product-containing fractions were combined and lyophilized. All lyophilized peptides were stored in a −20 °C freezer. A detailed synthesis scheme can be found in Scheme S1.

Cross-Linking. The self-assembling peptide MASP1 was first dissolved in 0.1 M MES buffer (pH 4.5) and allowed to form a hydrogel overnight before the postcross-linking chemistry was carried out. The MASP1 solution (3.5 mM, 90 μL) was initially activated by the addition of EDC/NHS (0.788 M, 10 μL) that was prepared beforehand in 0.1 M MES buffer (pH 4.5). The solution was vortexed for 5 s on the constant speed vortex mixer and settled for 10 min. To this solution was added either peptide cross-linkers or polyamines (25.2 mM for PCLs and spermines, 50 mM for EDBE, 50 μL) that were also prepared beforehand in 0.1 M MES buffer. The cross-linking reaction was allowed to continue for 2 h at room temperature after vortexing for 5 s. The final stoichiometry was made up to 25-times excess for EDC/NHS, and 4× excess for peptide cross-linkers or polyamines; the final concentration of MASP1 was 2.1 mM. All solutions added to MASP1 solutions were adjusted to pH 4.5 by 4 M HCl prior to mixing. After 2 h of cross-linking, the solutions were transferred into a dialysis unit, and dialyzed against 1 L of deionized water to remove the side products and salts (MWCO 2000, Thermo Scientific) for 24 h. The solution pH was checked by pH test paper and adjusted to ∼7 with 1 M NaOH if necessary.

Circular Dichroism. MASP1 was dissolved in 0.1 M MES buffer (pH 4.5) or Tris buffer (50 mM Tris-HCl, pH 7.5, 0.1 M NaCl, 100 mM $CaCl_2$) at a concentration of 400 μM. The solutions were loaded onto a 0.1 mm detachable cuvette and the spectra recorded on a JASCO spectropolarimeter. The mean residue ellipticity $[\theta]$ was calculated using the following equation

$$[\theta] = \frac{\theta}{c \cdot l \cdot n} \tag{1}$$

where θ is the measured ellipticity in mdeg, c is the concentration in dmol L^{-1} of the peptide calibrated by the absorbance of the tyrosine residue at 275 nm (1390 AU mol^{-1} cm^{-1}), l is the light path length of the cuvette in cm, and n is the number of amino acid residues.

Transmission Electron Microscopy. Specimens for TEM were prepared by loading 5 μL of solution on a copper grid covered with carbon film, and negatively stained using 2% uranyl acetate (Electron Microscopy Sciences, U.S.A.) following a previously reported procedure.[7,8,40] Cryogenic TEM specimens were prepared using a Vitrobot (FEI, U.S.A.): in brief, a drop of solution was first loaded onto a copper grid coated with lacey carbon film (Electron Microscopy Sciences, U.S.A.), followed by blotting using a piece of filter paper. The specimen was then plunged into liquid ethane to obtain a vitrified sample. All the samples were kept in liquid nitrogen before imaging. The detailed procedure for preparing cryo-TEM samples can be found in previous literature.[41] These samples were imaged on an FEI Tecnai 12 TWIN electron microscope operated at 100 kV. Digital micrographs were collected using a SIS Megaview wide angle camera.

Enzymatic Degradation Studies. The cross-linked hydrogels were treated with active MMP-2 (Merck Millipore, U.S.A.; active, human, recombinant, CHO cells) in testing buffer (final concentration was made up to 50 mM Tris-HCl, pH 7.5, 0.1 M NaCl, 100 mM $CaCl_2$) and incubated at room temperature for 6 h. Solutions were then loaded onto the stainless steel plate and mixed with 1% sinapinic acid for MALDI-ToF mass spectrometric analysis.

RESULTS AND DISCUSSION

Molecular Design. Figure 1 shows the rational design of the studied molecules illustrating two key design principles: (1) the reversible nature of the quick morphological transition process (Figures 1a,b and 2) the cross-linking of the assembled filaments using MMP-degradable sequences (Figure 1c). Our design rationale is to separate the molecular assembly event from the enzymatic cleavage reaction, with the aim of using the enzymatic cleavage to trigger the disassociation of the supramolecular filaments into individual building units. To accomplish this, we first create an amphiphilic peptide that has the ability to only self-assemble into 1D supramolecular filaments under acidic conditions (pH 4.5), where the cross-linking strategy can be applied to covalently lock the structure. These cross-linked filaments should then be stable under neutral conditions (pH 7.5) but will have the ability to quickly disassociate into individual molecules once the cross-linkers have been degraded by the targeted MMP.

The design of the self-assembling peptide was based on a miktoarm star motif with each arm possessing a specific function necessary to imbue the desired assembly properties.[42] Figure 1a shows the synthesized peptide MASP1, comprising three structural units: a β-sheet forming sequence plus three glutamic acid residues, an oligoproline segment, and a hydrophobic hydrocarbon. First, the peptide sequence of GNNQQNY was chosen to achieve the desired one-dimensionality. This seven-residue peptide is derived from the key amyloid-forming region of the yeast prion Sup35, known to adopt a parallel β-sheet secondary structure in the native protein.[43] Three glutamic acid residues were placed at the *C*-terminal of the peptide to impart the amphiphilic nature and the pH-responsiveness.

Second, an oligoproline unit is included to serve as a hydrophobic segment and, more importantly, is a key design feature to regulate the transition kinetics between the assembled filaments and other assembled/unassembled states. Oligoprolines are known as "molecular rulers" because of their high propensity to form the stable polyproline type II (PPII) helical secondary structure.[44,45] It has been reported that when packed in the crystal form, the center-to-center distance between PPII helices is ~6.6 Å,[44] a distance greater than the characteristic hydrogen bonding length in β-sheets (~4.7 Å). Consequently, if intermolecular hydrogen bonding between Sup35 segments occurs, the oligoproline segment must distort its natural PPII conformation to accommodate β-sheet formation (Figure 2b). We expect that this deformation of the PPII helical structure and its desire to return to its natural state will greatly accelerate the disassociation kinetics. Lastly, a short hydrocarbon tail (C_8) was introduced to provide increased hydrophobicity, enhancing the assembly potential of the designed molecules which were found to have poor assembly characteristics in its absence (vide infra). Details of the molecular synthesis, purification and characterization are described in Experimental Section and in the Supporting Information (SI; Figures S1−S5).

Characterization of Assemblies. The supramolecular filaments formed in MES buffer (~pH 4.5) can be clearly visualized using both transmission electron microscopy (TEM; Figure 2a) and cryogenic-TEM imaging techniques (Figure 2b). The diameter of the observed filaments is approximately 10 nm, with lengths on the order of tens of micrometers. Macroscopically, MASP1 forms a clear, self-supporting gel above 2 mM in MES buffer but presents as a fluidic liquid in Tris buffer (pH = 7.5; Figure 2c). The gel-to-solution transition was found to occur instantly when the solution pH was raised from 4.5 to ~7.0 by the addition of NaOH. TEM imaging showed no evidence of filamentous nanostructures existing in solutions aged overnight (Figure S6 in SI). It should be noted that the occasionally spotted irregular nanostructures in conventional TEM micrographs are not a dominant morphology and could just be a result of drying effects during TEM sample preparation. However, our Nile Red encapsulation experiments indeed reveal that MASP1 aqueous solution at pH 7.5 is still capable of sequestering the hydrophobic dye Nile Red, indicating that MASP1 could form some kind of micellar assemblies at the concentration of 2.1 mM (Figure S7). These micellar assemblies are expected to be in a dynamic equilibrium with the MASP1 monomers. A Thioflavin assay was also used to confirm that this self-assembling behavior is responsive to pH. Thioflavin T is a dye that exhibits enhanced fluorescent intensity when it binds to highly ordered amyloid structures.[46] After incubating the Thioflavin T with MASP1 in MES and Tris buffer, respectively, the dye fluoresced more intensively when mixed with MASP1 in MES buffer, where the filamentous structures were abundant in the solution; on the other hand, fluorescence of Thioflavin T was mostly quenched when mixed with MASP1 in Tris buffer (Figure 2d).

Circular dichroism (CD) studies on the MASP1 aqueous solutions exhibited typical absorptions of the polyproline II (PPII) helical conformation in both acidic and physiological conditions, as evidenced by a strong negative peak at 205 nm and a slightly positive peak around 225 nm (Figure 2e). This PPII helical conformation can be attributed to the oligoproline segment. Given the one dimensionality of the assembled nanostructures under acidic conditions, we speculate the formation of intermolecular hydrogen bonding among Sup35 segments but its existence cannot be directly confirmed via CD measurements as the β-sheet absorption was seemingly overwhelmed by the PPII signals. Wide angle X-ray scattering experiments were therefore performed, revealing the characteristic β-sheet spacing reflection (~4.7 Å; Figure S8 in SI). The existence of β-sheets strongly suggests the PPII helix (~6.6 Å minimum packing spacing) must be distorted within the filaments to accommodate the typical 4.7 Å spacing required for β-sheet formation. The slight difference in CD absorption (Figure 2d) might arise from this distortion of the PPII helix packing, combined with contributions from the β-sheet absorption.

We believe that the buried stress associated with the PPII deformation provides the impetus to rapidly disassociate the filaments into micellar assemblies and monomers at pH ~ 7. It has been shown by Meredith and co-workers that addition of a polyproline segment to the *C*-terminus of a polyglutamine sequence inhibits the formation of aggregation-prone β-sheets.[47] Indeed, removing the C_8 segment in our system, we found that the resultant conjugate (P_9G-Sup35) was unable to assemble into any well-defined structures at pH 4.5, possibly due to the β-sheet inhibitive nature imposed by the PPII-like

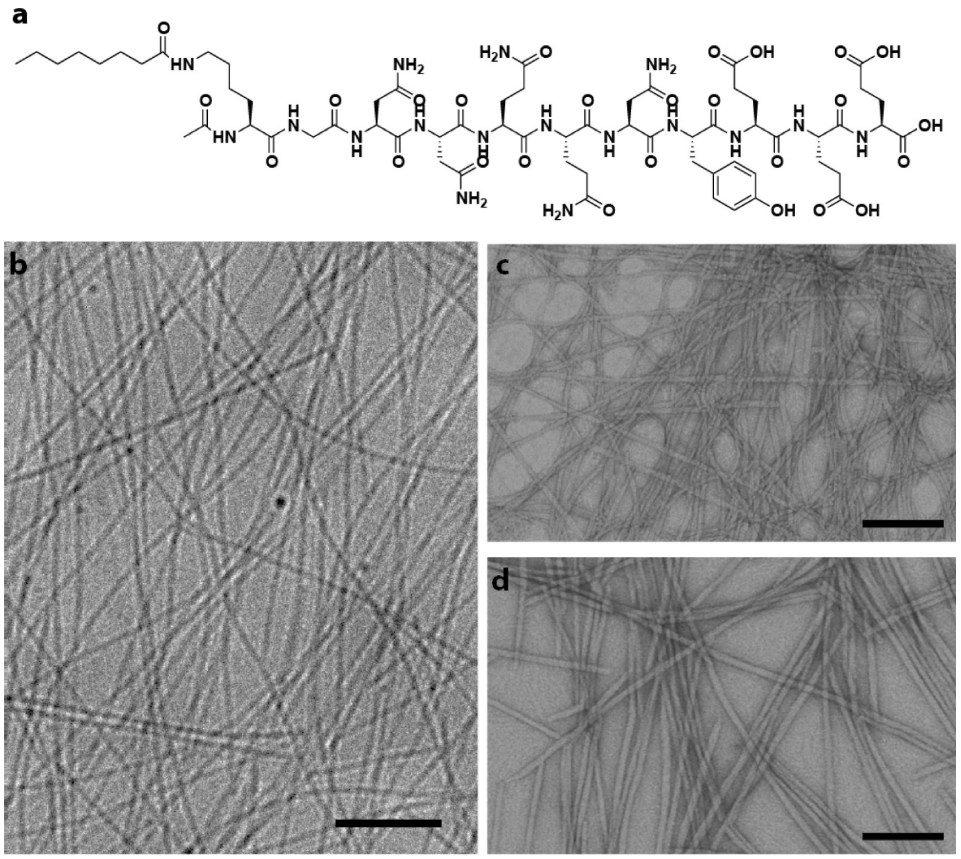

Figure 3. (a) Chemical structure of C_8-Sup35. Cryo-TEM (b) and TEM (c) micrographs of the filamentous structures formed by C_8-Sup35 in acidic conditions (pH 4.5) at 2.1 mM. (d) TEM micrograph of the filaments formed by C_8-Sup35 in pH ∼ 7 at 2.1 mM. All bars = 200 nm.

Scheme 1. Chemical Structures of the Four Cross-Linkers Designed/Used in the Study

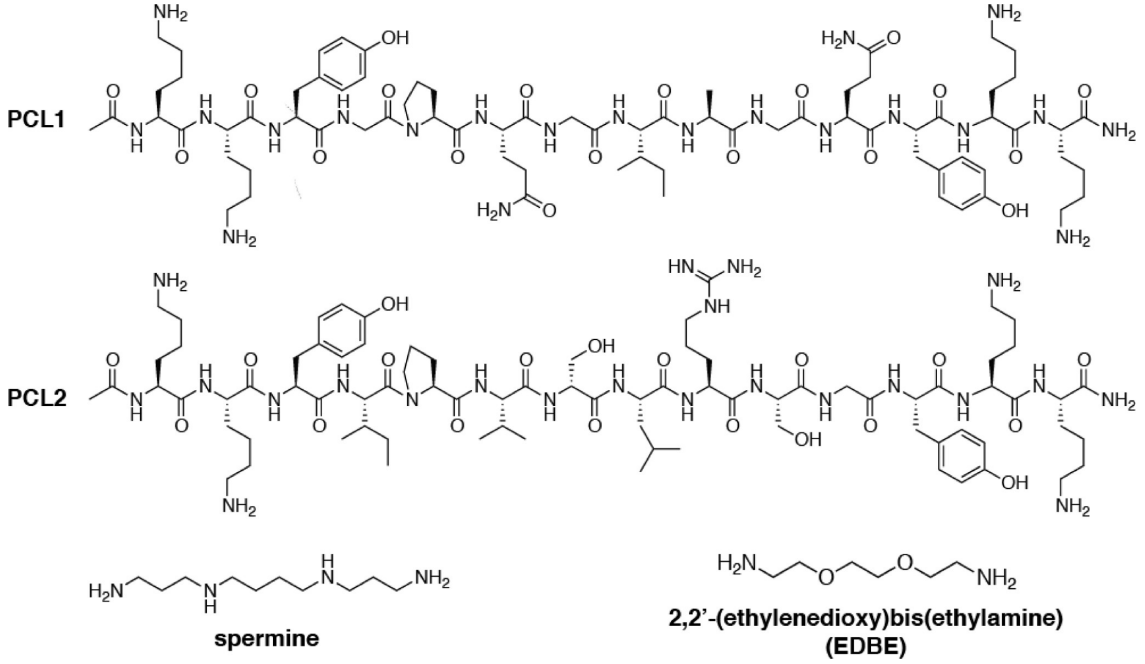

conformation adopted by the oligoproline segment (Figure S9 in SI). We also noted that the P_9G-Sup35 conjugate is capable of forming filamentous structures, only when the solution pH was lowered below 3. In contrast, the conjugate possessing no oligoproline (C_8-Sup35) can self-assemble into filamentous nanostructures at pH 4.5 (Figure 3a–c). However, these filaments do not rapidly disassociate upon raising the solution pH to around 7. After aging overnight, TEM examination still showed the existence of filaments as the dominant morphology (Figure 3d). Therefore, both the hydrocarbon and oligoproline

dx.doi.org/10.1021/bm500020j | *Biomacromolecules* 2014, 15, 1419–1427

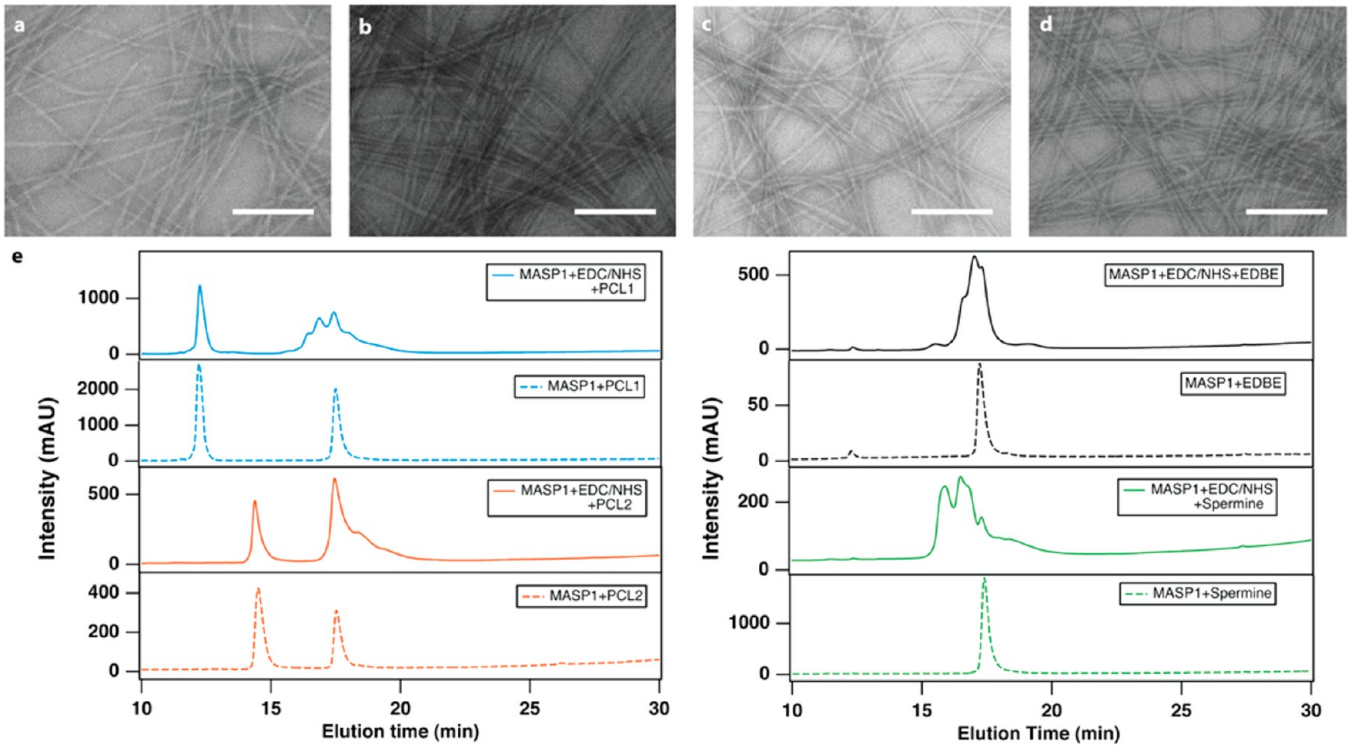

Figure 4. TEM micrographs of filaments after the postcross-linking treatment and qualitative analysis of cross-linked filaments. TEM micrographs of cross-linked filaments by PCL1 (a), PCL2 (b), EDBE (c), and spermine (d) at pH ~ 7. All scale bars = 200 nm. (e) Analytical HPLC traces of cross-linked filaments by PCL1 (blue) and PCL2 (orange; solid lines). In all cases, the corresponding peaks remain sharp and monodisperse in the chromatograms if EDC/NHS were not introduced to initiate the cross-linking chemistry (dashed lines).

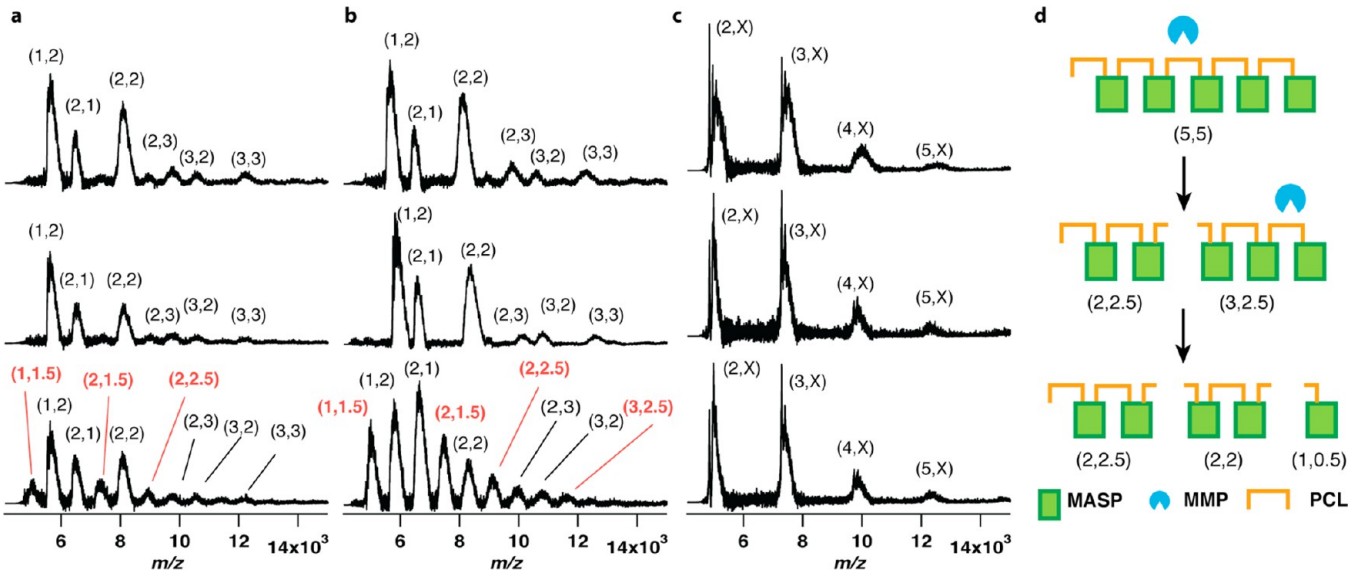

Figure 5. Enzymatic degradation studies on the cross-linked filaments in the presence of MMP-2. MALDI-ToF mass spectra of cross-linked filaments by PCL1 (a), PCL2 (b), and EDBE (c) before the enzymatic treatment (top spectrum), after the addition of Tris buffer (middle spectrum), and after 6 h of incubation with MMP-2 (bottom spectrum). Peaks are labeled with the (*m*,*n*) format, in which *m* represents the number of MASP1 molecules and *n* represents the number of the cross-linking molecules. (d) Schematic illustration of a representative pentamer of MASP1 linked with five PCLs and their possible degradation products after enzymatic cleavage of the PCLs.

segments are critical elements in the design of supramolecular filaments that possess rapid pH responsive behavior between pH 4.5 and 7.5.

Two MMP-2 peptide substrates, GPQG-IAGQ and IPVS-LRSG, were chosen for the design of the peptide cross-linkers PCL1 and PCL2 (the hyphen denotes the expected cleavage sites by MMP-2). Both sequences were reported to be degradable by MMP-2 with high specificity, with the latter yielding an ~8-fold higher value of k_{cat}/K_M than the former.[48] The sequence of PCL1 is actually derived from natural collagen.[48] Two lysine residues were placed at each terminal (Scheme 1) to react with the multiple carboxylic groups of the

dx.doi.org/10.1021/bm500020j | *Biomacromolecules* 2014, 15, 1419−1427

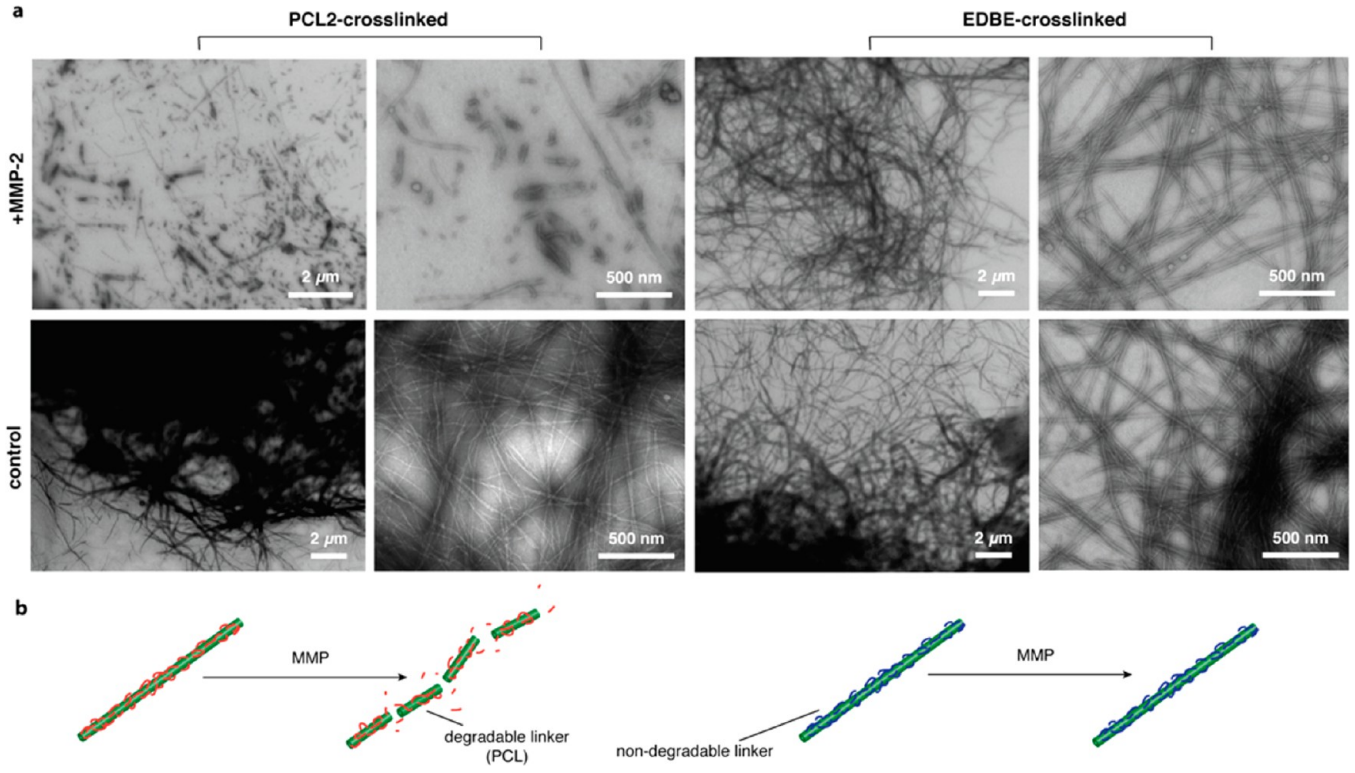

Figure 6. (a) TEM micrographs for the PCL2-cross-linked (top panels) and EDBE-cross-linked (bottom panels) filaments after 6 h incubation with MMP-2. The lengths of PCL2-cross-linked filaments were significantly reduced (top left panels) after incubation with MMP-2 for 6 h, while the EDBE-cross-linked filaments did not reveal any noticeable changes in filament length (bottom left panels). Both PCL2-cross-linked (top right panels) and EDBE-cross-linked filaments (bottom right panels) are very stable in the absence of MMP-2, and did not display any noticeable changes in filamentous structures 6 h after Tris buffer was added. (b) Schematic illustration of degradation pathways of supramolecular filaments cross-linked by MMP degradable and nondegradable linkers.

terminal glutamic acids on MASP1. Polyamines such as ethylenedioxybisethyamine (EDBE) and spermine (Scheme 1) were used as control cross-linkers for comparison. All cross-linking experiments were carried out in the assembly conditions (0.1 M MES buffer, pH 4.5) using 1-ethyl-3-[3-dimethylaminopropyl] carbodiimide (EDC) and *N*-hydroxysuccinimide (NHS) as initiators. The ratio of amines to carboxylic acids was chosen to be 4:1. After chemical cross-linking, the solution pH was adjusted to neutral conditions by adding NaOH to evaluate if this cross-linking strategy could preserve the filament structure. Figure 4a–d shows TEM images of the cross-linked filaments at pH ∼ 7, indicating that all four cross-linkers can successfully stabilize the supramolecular filaments. No apparent differences in morphology and length were observed between the cross-linked filaments and the non-cross-linked ones formed at pH 4.5, except that the cross-linked filaments seemed to have a greater tendency to bundle. It has been shown that the valency and the spacer distance between two adjacent reactive amines within the cross-linker play an important role in the cross-linking efficiency, leading to formation of different assembled morphologies.[49] However, under our experimental conditions (amine/acid = 4:1), the cross-linker identity did not appear to be a factor in the adopted morphology. Instead, the molecular design of MASP1 is the primary factor determining the assembled structures, suggesting that other cross-linkers specifically cleavable by different enzymes can also be used to stabilize the MASP1 filament without altering the assembly behavior of MASP1.

The cross-linking chemistry at the molecular level was first verified using analytical HPLC (Figure 4e). Without the addition of EDC/NHS initiators, mixtures of PCLs with MASP1 were eluted as two sharp, narrow peaks (dashed chromatograms in Figure 4e). MASP1 was consistently eluted after 17 min, while PCL1 and PCL2 were eluted after ∼12 and ∼14 min, respectively. EDBE and spermine were not observable due to their lack of absorbance at 220 nm (Figure 4e). Addition of the EDC/NHS initiators led to a broadening of the MASP1 elution peak (solid chromatograms in Figure 4e), clearly suggesting the existence of multiple products resulting from the cross-linking reaction.

MALDI-ToF mass spectrometry was then used to identify the molecular weights of the resultant chemical species. We found that these products can be assigned to species with varying numbers of MASP1 and PCLs (Figures 5a–c and S7 and Table S1 in SI). Because the molecular weights of EDBE or spermine were very small relative to that of MASP1, mass spectra of their cross-linked products only list the numbers of MASP1. These results also suggest that the cross-linking reaction did not transform the whole filament into one gigantic polymer. Actually, products containing large numbers of MASP1 and PCL were rarely observed in both MALDI and HPLC experiments. However, this lower degree of cross-linking is sufficient to stabilize the supramolecular filaments as TEM imaging shows that the cross-linked filaments are stable for at least five days at pH ∼ 7 (Figure S9 in SI). Quantification of the relative amount of different cross-linked products was not possible as the peak intensities in MALDI do not necessarily correlate to the absolute amount of the molecules present.

MMP-2 Degradation Experiments. The enzymatic degradation of the cross-linked MASP1 filaments was

dx.doi.org/10.1021/bm500020j | *Biomacromolecules* 2014, 15, 1419–1427

investigated by MALDI-ToF mass spectrometry. After 6 h incubation with MMP-2 (50 mM Tris, pH 7.5, 0.1 M NaCl, 10 mM $CaCl_2$), multiple new signals were observed for both PCL1- and PCL2-cross-linked filaments (Figure 5a−c, and Table S2 in SI). The molecular weight difference between these new species and the original masses in the untreated samples is typically around 800 Da, a value close to the molecular weights of the hydrolysis products of both PCL1 and PCL2 if they were cleaved at the expected sites (expected molecular weights of the hydrolysis products of PCL1: 818.92 and 805.96 Da; and PCL2: 876.05 and 850.02 Da). For cross-linked MASP1 molecules containing odd numbers of PCL residues, their degradation products can be assigned in the form of (m,n), for example (2,2.5; Figure 5d). However, one cannot distinguish if the signal (2,2) resulted from molecules containing two MASP1 linked by two PCLs, or from molecules containing two MASP1 linked by one PCL plus two PCL degradation segments (Figure 5d). For filaments cross-linked by EDBE, it is difficult to discern if chemical degradation takes place due to the limited resolution of the MS data obtained. These experiments reveal clearly that the peptide cross-linkers can be specifically degraded by the target MMP-2 at the desired cleavage sites at the molecular level.

To confirm that MMP-2 degradation of the cross-linked filaments had the desired effect, TEM imaging was performed on PCL-2 cross-linked filaments that had been treated for 6 h with MMP-2 (Figure 6). We found that most filaments had already dissociated, with only the occasional observation of some filamentous structures. In the absence of MMP-2, these cross-linked filaments were found to be very stable and did not exhibit any noticeable time-dependent morphological variation (Figure 6). The stability of the cross-linked filaments, combined with the observation of much shorter filaments after 6 h incubation with MMP-2, suggests that the MMP-2 cleavage reaction actually took place on the cross-linkers displayed on the nanofiber surfaces as shown in Figure 1c, not on the unassembled molecules in solution. It is very unlikely that the cross-linked filaments would first dissociate into monomeric forms which will then be degraded by MMP-2 given the structural stability of the cross-linked filaments.

CONCLUSION

In this work, we have reported a cross-linking strategy to construct MMP-degradable filaments formed by amyloid-derived amphiphilic peptides. One key design feature is the incorporation of an oligoproline sequence that allows for rapid disassociation of the assembled β-sheet rich nanostructures upon degradation of the peptide cross-linkers. We also show that the peptide substrates displayed on the filament surfaces are still accessible for specific MMP cleavage. Notably, the use of four structurally different cross-linkers did not alter the assembled morphology, suggesting the possibility of using other peptide cross-linkers for different types of enzymes. Because the assembly process is well separated from the incorporation of MMP degradability, peptide substrates of other proteases could be chosen as a potential cross-linker to stabilize the MASP1 filaments. The cross-linked filaments may find their use as individual carriers for drugs or imaging agents because of their improved stability during circulation and also of their enzyme-induced instability once reaching their targets. Hydrogels of the cross-linked filaments could be potentially used as scaffolding materials for cell and protein delivery, or for studying cell differentiation and migration.

In order to develop peptide-based supramolecular filaments and hydrogels with degradation kinetics controlled by the targeted proteases (e.g., MMPs) for ultimate biomedical applications, two important issues need to be addressed: First, the specificity of the chosen peptide substrates to the targeted protease must be quantified experimentally. The two peptide substrates used in our work, one derived from natural collagen and the other screened from a peptide library, are highly specific to the MMP-2 in the soluble form, however, it is not clear how much their specificity is altered when displayed on the filament surfaces. Although our MALDI experiments reveal that the cleavage sites of both PCL1 and PCL2 remain unchanged in our studies, future work should be pursued to quantify the specificity by directly measuring the value of k_{cat}/K_M. The second important issue is the toxicity of all the chemicals involved in the cross-linking reactions. Our recent experiments reveal that, although the designed peptide MASP1 do not possess any potential toxicities to cells, the EDC/NHS initiators used in our studies are highly toxic. Therefore, these toxic initiators must be completely removed via extensive dialysis. Alternatively, other cross-linking methods such as Michael-type addition,[50,51] or enzyme-catalyzed reactions[52] could be used to covalently fix the peptide supramolecular filaments. Despite these challenges, we believe that our reported system present a new platform for the design of enzymatically degradable materials, and this platform can be potentially extended to construct filaments responsive not only to other members of the MMP family, but also to other types of proteases or enzymes.

ASSOCIATED CONTENT

Supporting Information

Details of synthesis route, molecular characterization, degradation products, X-ray scattering data, and additional TEM images. This material is available free of charge via the Internet at http://pubs.acs.org.

AUTHOR INFORMATION

Corresponding Author

*E-mail: hcui6@jhu.edu.

Notes

The authors declare no competing financial interest.

ACKNOWLEDGMENTS

We thank the Johns Hopkins University (JHU) for the New Faculty Startup grant, and the National Institute of Health (NIH) for funding Y.L. (R25 CA153952) and A.C. (T-32 CA130840). We thank the JHU Integrated Imaging Center (IIC) for the use of the TEM facility, and the JHU Department of Chemistry Mass Spectrometry facility for MALDI-ToF analysis (NSF CHE-0840463). We also thank Prof. Kalina Hristova (MSE, JHU) for the use of the CD instrument. Use of the Advanced Photon Source was supported by the U.S. Department of Energy, Basic Energy Sciences, Office of Science, under Contract No. DE-AC02-06CH11357. Use of BioCARS was also supported by the National Institutes of Health, National Institute of General Medical Sciences Grant P41GM103543 (formerly National Center for Research Resources P41RR007707).

REFERENCES

(1) Hartgerink, J. D.; Beniash, E.; Stupp, S. I. *Science* **2001**, *294*, 1684−1688.
(2) Yu, Y. C.; Berndt, P.; Tirrell, M.; Fields, G. B. *J. Am. Chem. Soc.* **1996**, *118*, 12515−12520.
(3) Hauser, C. A. E.; Zhang, S. G. *Chem. Soc. Rev.* **2010**, *39*, 2780−2790.
(4) Jonker, A. M.; Lowik, D.; van Hest, J. C. M. *Chem. Mater.* **2012**, *24*, 759−773.
(5) Branco, M. C.; Sigano, D. M.; Schneider, J. P. *Curr. Opin. Chem. Biol.* **2011**, *15*, 427−434.
(6) Hamley, I. W. *Soft Matter* **2011**, *7*, 4122−4138.
(7) Cheetham, A. G.; Zhang, P. C.; Lin, Y. A.; Lock, L. L.; Cui, H. G. *J. Am. Chem. Soc.* **2013**, *135*, 2907−2910.
(8) Zhang, P. C.; Cheetham, A. G.; Lin, Y. A.; Cui, H. *ACS Nano* **2013**, *7*, 5965−5977.
(9) Nowak, A. P.; Breedveld, V.; Pakstis, L.; Ozbas, B.; Pine, D. J.; Pochan, D.; Deming, T. J. *Nature* **2002**, *417*, 424−428.
(10) Tang, C.; Smith, A. M.; Collins, R. F.; Ulijn, R. V.; Saiani, A. *Langmuir* **2009**, *25*, 9447−9453.
(11) Soukasene, S.; Toft, D. J.; Moyer, T. J.; Lu, H. M.; Lee, H. K.; Standley, S. M.; Cryns, V. L.; Stupp, S. I. *ACS Nano* **2011**, *5*, 9113−9121.
(12) Branco, M. C.; Pochan, D. J.; Wagner, N. J.; Schneider, J. P. *Biomaterials* **2009**, *30*, 1339−1347.
(13) Haines-Butterick, L.; Rajagopal, K.; Branco, M.; Salick, D.; Rughani, R.; Pilarz, M.; Lamm, M. S.; Pochan, D. J.; Schneider, J. P. *Proc. Natl. Acad. Sci. U.S.A.* **2007**, *104*, 7791−7796.
(14) Cui, H. G.; Webber, M. J.; Stupp, S. I. *Biopolymers* **2010**, *94*, 1−18.
(15) Stupp, S. I. *Nano Lett.* **2010**, *10*, 4783−4786.
(16) Zhang, S. G. *Nat. Biotechnol.* **2003**, *21*, 1171−1178.
(17) Zhao, F.; Ma, M. L.; Xu, B. *Chem. Soc. Rev.* **2009**, *38*, 883−891.
(18) Lin, R.; Cheetham, A. G.; Zhang, P. C.; Lin, Y. A.; Cui, H. G. *Chem. Commun.* **2013**, *49*, 4968−4970.
(19) Lock, L. L.; Lacomb, M.; Schwarz, K.; Cheetham, A. G.; Lin, Y. A.; Zhang, P.; Cui, H. *Faraday Discuss.* **2013**, 285−301.
(20) Black, M.; Trent, A.; Kostenko, Y.; Lee, J. S.; Olive, C.; Tirrell, M. *Adv. Mater.* **2012**, *24*, 3845−3849.
(21) Rudra, J. S.; Sun, T.; Bird, K. C.; Daniels, M. D.; Gasiorowski, J. Z.; Chong, A. S.; Collier, J. H. *ACS Nano* **2012**, *6*, 1557−1564.
(22) Lutolf, M. P.; Hubbell, J. A. *Nat. Biotechnol.* **2005**, *23*, 47−55.
(23) Liu, Y.; Terrell, J. L.; Tsao, C. Y.; Wu, H. C.; Javvaji, V.; Kim, E.; Cheng, Y.; Wang, Y. F.; Ulijn, R. V.; Raghavan, S. R.; Rubloff, G. W.; Bentley, W. E.; Payne, G. F. *Adv. Funct. Mater.* **2012**, *22*, 3004−3012.
(24) Hirst, A. R.; Roy, S.; Arora, M.; Das, A. K.; Hodson, N.; Murray, P.; Marshall, S.; Javid, N.; Sefcik, J.; Boekhoven, J.; van Esch, J. H.; Santabarbara, S.; Hunt, N. T.; Ulijn, R. V. *Nat. Chem.* **2010**, *2*, 1089−1094.
(25) Gao, Y.; Shi, J. F.; Yuan, D.; Xu, B. *Nat. Commun.* **2012**, *3*, 1−8.
(26) Guilbaud, J. B.; Vey, E.; Boothroyd, S.; Smith, A. M.; Ulijn, R. V.; Saiani, A.; Miller, A. F. *Langmuir* **2010**, *26*, 11297−11303.
(27) Yang, Z. M.; Ma, M. L.; Xu, B. *Soft Matter* **2009**, *5*, 2546−2548.
(28) Rodriguez, A. R.; Kramer, J. R.; Deming, T. J. *Biomacromolecules* **2013**, *14*, 3610−3614.
(29) Giano, M. C.; Pochan, D. J.; Schneider, J. P. *Biomaterials* **2011**, *32*, 6471−6477.
(30) Galler, K. M.; Aulisa, L.; Regan, K. R.; D'Souza, R. N.; Hartgerink, J. D. *J. Am. Chem. Soc.* **2010**, *132*, 3217−3223.
(31) Webber, M. J.; Newcomb, C. J.; Bitton, R.; Stupp, S. I. *Soft Matter* **2011**, *7*, 9665−9672.
(32) Jun, H. W.; Yuwono, V.; Paramonov, S. E.; Hartgerink, J. D. *Adv. Mater.* **2005**, *17*, 2612−2617.
(33) Chau, Y.; Luo, Y.; Cheung, A. C. Y.; Nagai, Y.; Zhang, S. G.; Kobler, J. B.; Zeitels, S. M.; Langer, R. *Biomaterials* **2008**, *29*, 1713−1719.
(34) Dehsorkhi, A.; Hamley, I. W.; Seitsonen, J.; Ruokolainen, J. *Langmuir* **2013**, *29*, 6665−6672.
(35) Ma, Q. G.; Remsen, E. E.; Kowalewski, T.; Schaefer, J.; Wooley, K. L. *Nano Lett.* **2001**, *1*, 651−655.
(36) Ma, Q. G.; Wooley, K. L. *J. Polym. Sci., Part A: Polym. Chem.* **2000**, *38*, 4805−4820.
(37) Zhang, Y.; Li, N.; Delgado, J.; Gao, Y.; Kuang, Y.; Fraden, S.; Epstein, I. R.; Xu, B. *Langmuir* **2012**, *28*, 3063−3066.
(38) Zhang, Y.; Zhou, R.; Shi, J. F.; Zhou, N.; Epstein, I. R.; Xu, B. *J. Phys. Chem. B* **2013**, *117*, 6566−6573.
(39) Kessenbrock, K.; Plaks, V.; Werb, Z. *Cell* **2010**, *141*, 52−67.
(40) Lock, L. L.; Cheetham, A. G.; Zhang, P. C.; Cui, H. G. *ACS Nano* **2013**, *7*, 4924−4932.
(41) Cui, H.; Hodgdon, T. K.; Kaler, E. W.; Abezgauz, L.; Danino, D.; Lubovsky, M.; Talmon, Y.; Pochan, D. J. *Soft Matter* **2007**, *3*, 945−955.
(42) Lin, Y. A.; Ou, Y. C.; Cheetham, A. G.; Cui, H. *ACS Macro Lett.* **2013**, *2*, 1088−1094.
(43) Nelson, R.; Sawaya, M. R.; Balbirnie, M.; Madsen, A. O.; Riekel, C.; Grothe, R.; Eisenberg, D. *Nature* **2005**, *435*, 773−778.
(44) Cowan, P. M.; McGavin, S.; North, A. C. T. *Nature* **1955**, *176*, 1062−1064.
(45) Arora, P. S.; Ansari, A. Z.; Best, T. P.; Ptashne, M.; Dervan, P. B. *J. Am. Chem. Soc.* **2002**, *124*, 13067−13071.
(46) Levine, H. *Protein Sci.* **1993**, *2*, 404−410.
(47) Darnell, G.; Orgel, J.; Pahl, R.; Meredith, S. C. *J. Mol. Biol.* **2007**, *374*, 688−704.
(48) Turk, B. E.; Huang, L. L.; Piro, E. T.; Cantley, L. C. *Nat. Biotechnol.* **2001**, *19*, 661−667.
(49) Cui, H. G.; Chen, Z. Y.; Wooley, K. L.; Pochan, D. J. *Macromolecules* **2006**, *39*, 6599−6607.
(50) Cellesi, F.; Tirelli, N.; Hubbell, J. A. *Biomaterials* **2004**, *25*, 5115−5124.
(51) Patterson, J.; Hubbell, J. A. *Biomaterials* **2010**, *31*, 7836−7845.
(52) Bakota, E. L.; Aulisa, L.; Galler, K. M.; Hartgerink, J. D. *Biomacromolecules* **2011**, *12*, 82−87.